Structure and Properties for Conterminously Linked Polymer of Copoly(amic acid) with Triallyl Isocyanurate and Bismaleimide

Chien-Lin Huang,[1] Chun-Shan Wang,[1] Tsu-Shang Leu[2]

[1]Department of Chemical Engineering, National Cheng Kung University, Tainan, Taiwan
[2]Department of Biological and Cosmetic Application Engineering, Yung-Ta Institute of Technology and Commerce, Linlo, Pingtung, Taiwan

ABSTRACT: The copoly(amic acid)s were prepared from two various diamines 2,2′-bis (4-aminophenoxy phenyl) hexafluoropropane or 2,2′-bis (4-aminophenoxy phenyl) propane and amine-terminated oligosiloxane, respectively, with aromatic tetracarboxylic dianhydride (3,3′,4,4′-benzophenone tetracarboxylic dianhydride). The resulted copoly(amic acid) with various mole ratio of triallyl isocyanurate (TAIC)/4,4′-bismaleimidophenylmethane (BMI) were subsequently thermally imidized to the corresponding copolyimides. These polymers were characterized using viscometer, differential scanning calorimetry, thermogravimetric analyses, dynamic mechanical analysis (DMA), dielectric analyzer, and scanning electron microscope. The dielectric constant (D_K) and dissipation factor (D_f) of copolyimides with TAIC/BMI were much lower than that of copolyimides without TAIC/BMI. Furthermore, the formation of copolyimides also would enhance their thermal stability and solubility. DMA of copolymers showed only a glass transition temperature (T_g), indicating a random structure and an amorphous state. The morphology of copolyimides revealed no phase separation. This indicates that the homogeneous state has been achieved in this coreaction system. © 2007 Wiley Periodicals, Inc. J Appl Polym Sci 107: 3280–3290, 2008

Key words: copolyimide; thermal stability; random structure

INTRODUCTION

High-performance polymers are very useful in highly demanding environments to provide special properties. They are employed as resins in advanced composites and in electronics. The articles had been published and updated in our study.[1–4] Addition and condensation imide resins are two different types of imides available for high-performance matrix applications. Addition polyimides are usually low-molecular-weight resins (e.g. bismaleimide) containing unsaturated moieties for subsequent crosslinking reactions. Owing to the high crosslinking density, addition polyimides generally possess high stiffness. Condensation polyimides (i.e. polyimides), in particular those derived from fully aromatic monomers, represent the most important class of high temperature polymers. These materials have a number of outstanding properties,[5–10] and have been widely used in electronic applications, membranes for gas separation, structural adhesives, sealants and as matrices for high-perform-ance advanced nanocomposite materials.[11,12] However, most polyimides suffer from processing problems because of their insolubility/infusibility, and the evolution of volatiles during the ring formation. High-performance polyimides are used in the fabrication of microelectronic devices as interdielectric and passivation layers, owing to relatively high thermal stability and excellent electrical properties. Modified structures with flexible (ether or siloxane) linkages[13,14] between aromatic rings or with bulky pendant (heterocyclic or branch) groups[15,16] have provided improvement in solubility,[17–26] which noncoplanar (i.e. three-dimensional)[27] and asymmetric (or zigzag) structure[28–36] have also found to be quite effective in improving the solubility of polyimides. Moreover, the introduction of the phenylethynyl group as an end-capping agent in low-molecular-weight imide oligomers has greatly improved the processability.[37–39]

Epoxy resins modified with bismaleimide through reaction and blending have been reported to show good physical and chemical properties.[40–42] Additionally, the use of a reactive compound triallyl isocyanurate (TAIC) to improve the particulate morphology of polymer.[43,44] In our previous work,[45] the coreaction of epoxy with TAIC/4,4′-bismaleimidophenylmethane (BMI), and the resultant yield a homogeneous system. In this study, copoly(amic acid)

was synthesized from a 3,3′,4,4′-benzophenone tetra-carboxylic dianhydride (BTDA) with a mixture of two diamines (i.e. BAPP/ATOS and BAFP/ATOS). The resulted copoly(amic acid) was subsequently blended with various mole ratios of TAIC/BMI, and thermally imidized to the corresponding copolyimide. It was reasoned that the introduction of the damines 2,2′-bis (4-aminophenoxy phenyl) hexafluoropropane (BAFP) and 2,2′-bis (4-aminophenoxy phenyl) propane (BAPP), containing hexafluoroisopropylidene with ether linkage and flexible siloxane unit that could reduce the stiffness of the polymer backbone and enhance the solubility of the resulting copolyimides. Furthermore, the interchain interaction of amine-terminated imide with TAIC/BMI could yield larger free volume of polymer and hence improve the dielectric property of copolyimides. This article also explores the relationship between the structure, morphology, and properties of these systems.

EXPERIMENTAL

Materials

2,2-Bis(4-hydroxy phenyl) propane or bisphenol A (BPA, Acros, Belgium), 2,2-bis(4-hydroxy phenyl) hexafluoropropane or bisphenol AF (BPAF, (Chriskev), *p*-chloronitrobenzene (Acros), anhydrous potassium carbonate (Showa, Tokyo, Japan), hydrazine monohydrate (Acros), and 10% palladium on activated charcoal (TCI, Tokyo, Japan) were used. Amine-terminated oligosiloxane (ATOS, weight average molecular is 900, Shin-Etsu, Japan), 3,3′,4,4′-benzophenone tetracarboxylic dianhydride (BTDA, Acros), triallyl isocyanurate (TAIC, Aldrich), 4,4′-bismaleimidophenylmethane or bismaleimide (BMI, Aldrich, Milwaukee, WI), *N,N*-dimethylacetamide (Tedia), *N*-methyl-2-pyrrolidinone (NMP, Tedia), tetrahydrofuran (Tedia). The solvent (NMP) for copolyimide synthesis was dehydrated with CaH_2 and then distilled before being stored in 4-Å molecular sieves. Triphenylphosphine (Ph$_3$P) was obtained from TCI, and that was used as an accelerator. All the monomers were commercial products (LC grade) and used without further purification.

Measurements

Differential scanning calorimeter (DSC; Perkin-Elmer DSC-7) measurements were used in this study. Samples of ∼ 5–10 mg in weight were sealed in hermetic aluminum pans and scanned in the calorimeter at a heating rate of 10°C/min from 30 to 350°C under N_2 atmosphere. For dynamic scanning, calibration of the calorimeter was conducted for the heating rate using an indium standard. Thermogravimetric analyses (TGA) were performed on a Perkin-Elmer TGA-7 thermal analyzer using a heating rate of 20°C/min in N_2

at a purge pressure of 25 psi within the temperature range of 30–800°C. Dynamic mechanical analysis (DMA) was performed on a Perkin–Elmer DMA-7 thermal analyzer system. A sample 15-mm length (measuring system display sample height, it was decided from zero), 3 mm in width, and ∼ 42 μm in depth was used. The modulus and glass transition temperature (T_g) values were taken as the peak of tan δ in the heat flow curves were studied when the sample was subjected to temperature scan mode with a extension measuring system (use stainless steel extension kit) at a programmed heating rate of 10°C/min in a frequency of 1 Hz. ^{1}H NMR spectra were registered using a Bruker Avance-600 spectrometer using DMSO-d_6 as a solvent. Elemental analyses were carried out with a Heraeus CHN-Rapid elemental analyzer. Fourier transform infrared (FTIR) spectra were recorded on a 8100-type spectrometer with KBr pellets, and spectra in the optical range of 400–4000 cm^{-1} were obtained by averaging 32 scans at a resolution of 4 cm^{-1}. The dielectric constant and dissipation factor were determined by the bridge method with a RF impedance/material Analyzer at 1 MHz. The applied voltage was 1 V and was maintained at room temperature in N_2 by the two parallel plate mode. The specimens (1 × 1 cm^2 × 3 mm thickness) were subjected to vacuum pretreatment of 1–3 mmHg at 100°C for 8 h to eliminate the absorbed water. A Hitachi S 4200 scanning electron microscope (SEM) was employed to examine the morphology of samples fractured cryogenically in liquid nitrogen. The fracture surfaces were vacuum-coated with gold.

Syntheses of 2,2′-bis(4-nitrophenoxy phenyl) propane, 2,2′-bis(4-nitrophenoxy phenyl) hexafluoropropane, BAPP, and BAFP

The 2,2′-bis(4-nitrophenoxy phenyl) propane (BNPP) and BAPP were synthesized according to literatures described in Ref. 46. Another 2,2′-bis(4-nitrophenoxy phenyl) hexafluoropropane (BNFP) and BAFP were synthesized analogously, the element analyses for BNFP; C = 56.06%, H = 2.77%, N = 4.84% (theoretically) and C = 55.91%, H = 2.80%, N = 4.80% (experimentally), and the element analyses for BAFP; C = 62.55%, H = 3.86%, N = 5.51% (theoretically) and C = 62.17%, H = 3.87%, N = 5.35% (experimentally).

Copoly(amic acid) synthesis (1) PAA (BAPP-ATOS/BTDA) and (2) PAF (BAFP-ATOS/BTDA)

Into a 250-mL four-necked round-bottom separable flask equipped with an addition funnel and a high-purity N_2 inlet, a solution of diamine (including ATOS and BAPP, mole ratio is 1 : 4, 2.2140 g of ATOS and 4.0344 g of BAPP were mixed) in 50 g of NMP was charged, then 3.7638 g of BTDA was
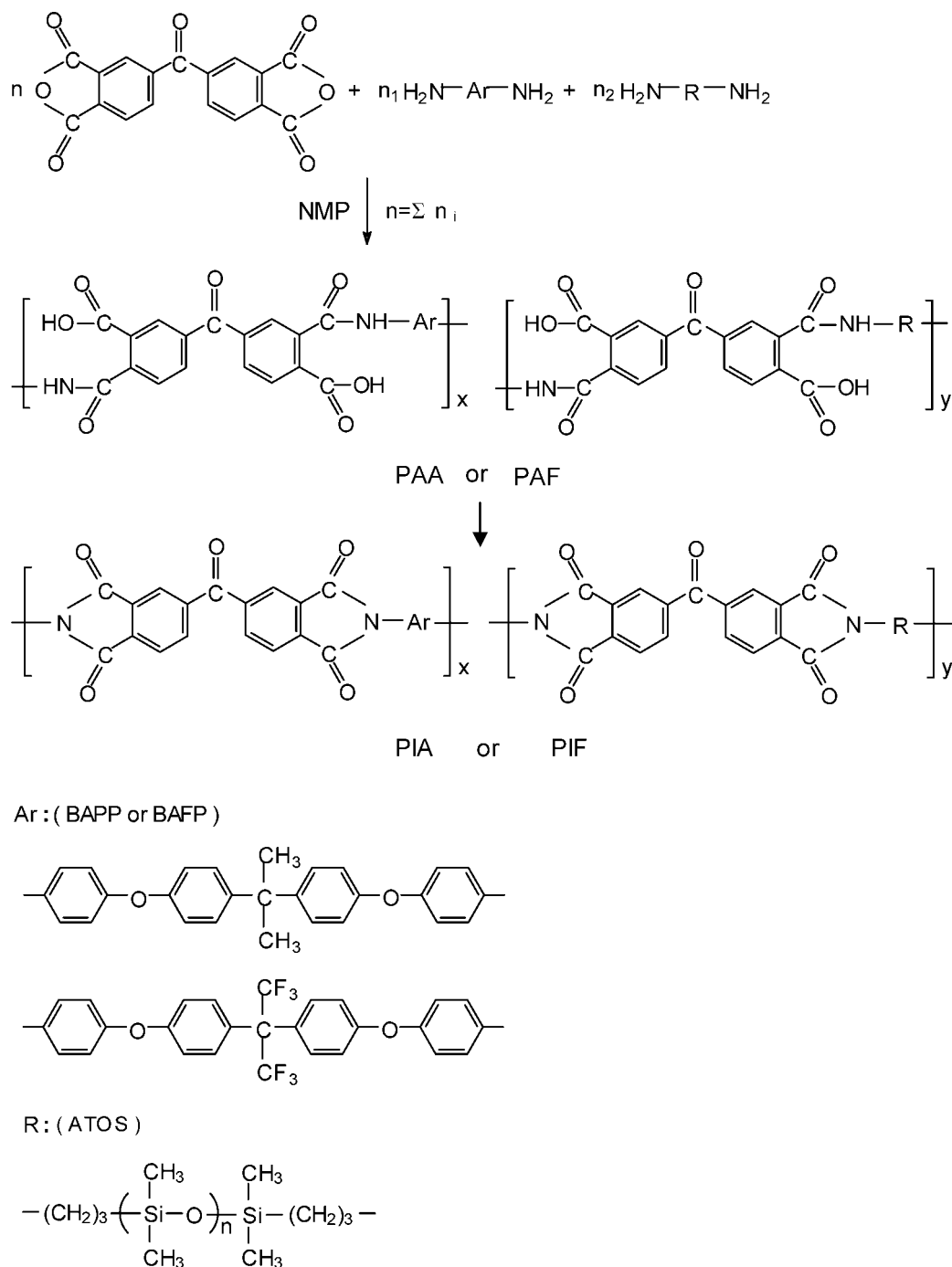
Scheme 1 The copolyimide (PIA or PIF) was prepared from their corresponding copoly(amic acid) (PAA or PAF).

added all at once. The mole ratio and solid content in solvent of diamine/dianhydride mixture were equally equivalent and 20 wt %, respectively, see eq. (1). For solid content in solvent;

$$\frac{m\left[(\sum x_i M_i)_{\text{diamine}} + M_{\text{dianhyd}}\right]}{W_s} = 0.2 \quad (1)$$

Here, m is the mole, x_i is the mole fraction of component i, M_i is the molecular weight of component i, W_s is the weight of solvent (50 g). The reaction mixture was stirred at room temperature in N_2 atmosphere affording a viscous copoly (amic acid) solution after 4 h. Another copoly(amic acid), PAF (with BAFP-ATOS/BTDA) was prepared analogously. The reaction is shown in Scheme 1.
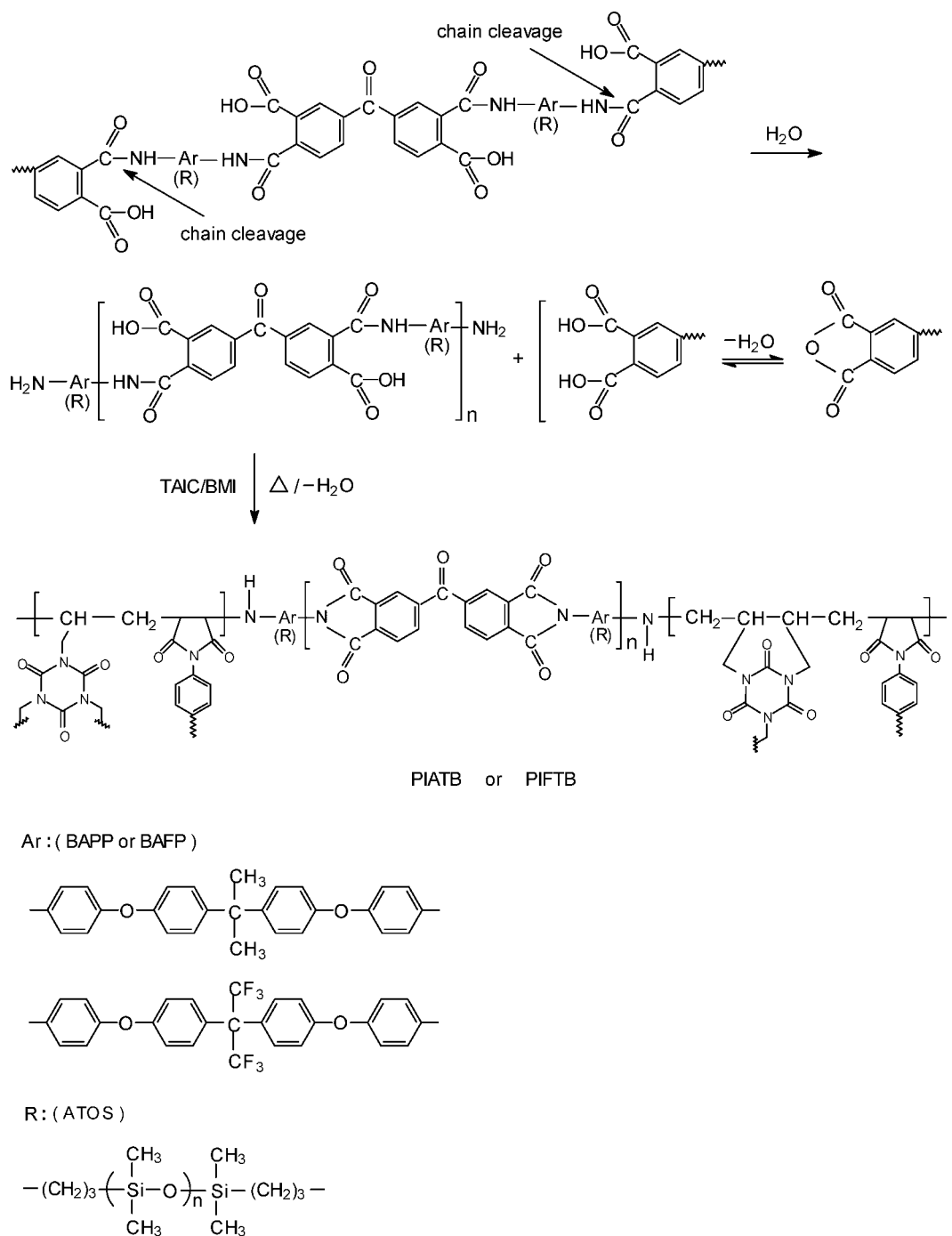
Scheme 2 The interaction of amine-terminated poly(amic acid) with TAIC/BMI.

Copolyimide and film casting, (1) PIA (from PAA) and PIF (from PAF) (2) PIATB (from PAA with TAIC/BMI) and PIFTB (from PAF with TAIC/BMI)

The PAA and TAIC/BMI (mole ratio = 2/3) at an equivalent amount with 0.2% Ph$_3$P were mixed together, see eq. (2) (e.g. 10 wt %)

$$\frac{n(\sum x_i M_i)_{\text{TAIC/BMI}}}{n(\sum x_i M_i)_{\text{TAIC/BMI}} + W_{\text{PAA}}} = 0.1 \qquad (2)$$

where n is the mole, x_i is the mole fraction of component i, M_i is the molecular weight of component i, and W_{PAA} is the weight of copoly(amic acid). TAIC (0.7072 g) and BMI (1.5251 g) were added to the aforementioned solution of W_{PAA} (20 g). The reaction mixture was spread (with film casting apparatus) on a heatproof glass plate and dried at 60°C for 12 h in a forced air oven. The film on glass was then converted to copolyimide by heating in air at 100°C for 2 h, 200°C for 1 h, 250°C for 1 h, and 300°C for 2 h.

TABLE I
Synthesis of Copolyimides from Various Component, Composition Systems, and Thermal Stability, Mechanical and Electric Properties

Polymer	$\eta_r{}^a$	$[\eta]_{exp}{}^b$ (dL/g)	$[\eta]_{cal}{}^c$ (dL/g)	$T_g{}^d$ (°C)	$T_d{}^e$ (°C)	Char yield^f (%)	$D_k{}^g$ (U)	$D_f{}^h$ (mU)	Modulus^i (10^8 Pa)
PIA	1.053	0.44	0.39	213	520	61.5	3.01	14.3	3.6
PIATB10	1.056	0.47	0.41	225	530	51.1	2.93	11.5	4.2
PIATB20	1.067	0.52	0.49	247	521	58.2	2.84	10.2	3.8
PIATB30	1.115	0.88	0.86	284	516	63.2	2.78	9.6	3.5
PIATB40	1.118	1.02	0.89	293	483	56.8	2.72	8.4	3.4
PIATB50	1.126	1.11	0.95	352	484	52.7	2.70	7.8	2.6
PIF	1.072	0.56	0.53	192	535	47.4	2.87	13.2	2.8
PIFTB10	1.146	1.15	1.11	200	556	51.4	2.82	11.4	3.8
PIFTB20	1.162	1.24	1.24	219	529	49.6	2.74	9.8	3.4
PIFTB30	1.119	1.33	1.29	224	525	54.5	2.71	8.7	2.6
PIFTB40	1.208	1.58	1.60	236	506	52.2	2.65	7.6	2.4
PIFTB50	1.253	1.97	1.98	296	502	51.6	2.62	7.1	2.1

^{a} 0.14 g/dL in concentrated NMP at 30°C.
^{b} The solution (in concentrated NMP, 0.12–0.16 g/dL, taking five points) was measured at 30°C, by extrapolation to zero concentration, yielding $[\eta]_{exp}$, that is $\left[\frac{\ln \eta_r}{c}\right]_{c \to 0} = [\eta]_{exp}$.
^{c} Calculated from eq. (4), taking average concentration value (0.14 g/dL, from 0.12 to 0.16 g/dL), the full equation may be written as $\left[\frac{\ln \eta_r}{c}\right] = \frac{1}{2c}\eta_r(\eta_r - 1)(3 - \eta_r) = [\eta]_{cal}$.
^{d} T_g measured by DMA.
^{e} Five weight percent decomposition temperature under nitrogen atmosphere.
^{f} Char yield at 800°C under nitrogen atmosphere.
^{g} Dielectric constant measured at 1 MHz, room temperature.
^{h} Dissipation factor measured at 1 MHz, room temperature.
^{i} The modulus values at 75°C were observed.

The film was cooled to room temperature and stripped from the plate by soaking in water. Another copolyimide film, PAF with TAIC/BMI (PIFTB system) was prepared analogously. The reaction is shown in Schemes 1 and 2.

Sample code

The sample codes for diamine ATOS-based copolyimides are designated PIA and PIF, respectively, as shown in Scheme 1. PI stands for copolyimide, A (or F) stands for BAPP (or BAFP). However, for the modified copolyimides are designated as PIATB-XY and PIFTB-XY, respectively. The number of XY after the dash is the weight percentage of TAIC/BMI-modified copolyimide. For the systems, TAIC and BMI were applied to the starting mixture with PAA and PAF, as shown in Scheme 2 and Table I.

RESULTS AND DISCUSSION

Synthesis of monomer

The monomers (BNPP, BNFP, BAPP, and BAFP) were synthesized according to our laboratory method. All monomers, expect elemental analysis, and the structures of diamines BAPP and BAFP were confirmed by NMR and were in agreement with the proposed structures. Figure 1 shows the ^{1}H-NMR spectra of BAPP and BAFP. The characteristic peaks for BAPP of the aromatic Hs at 6.58–7.11

ppm, amine at 4.95 ppm, and aliphatic Hs at 1.56 ppm is observed. The ratio of integration area of the aromatic Hs : amine Hs : aliphatic Hs is 3.83 : 0.98 : 1.50 = 3.91 : 1.00 : 1.53, which agrees with the theoretical value of 16 : 4 : 6 = 4.0 : 1.0 : 1.5, whereas the aliphatic Hs peak at around 1.56 ppm have disappeared in the BAFP spectrum. The characteristic peaks of the aromatic Hs at 6.60–7.25 ppm and amine at 5.05 ppm is observed. The ratio of integra-
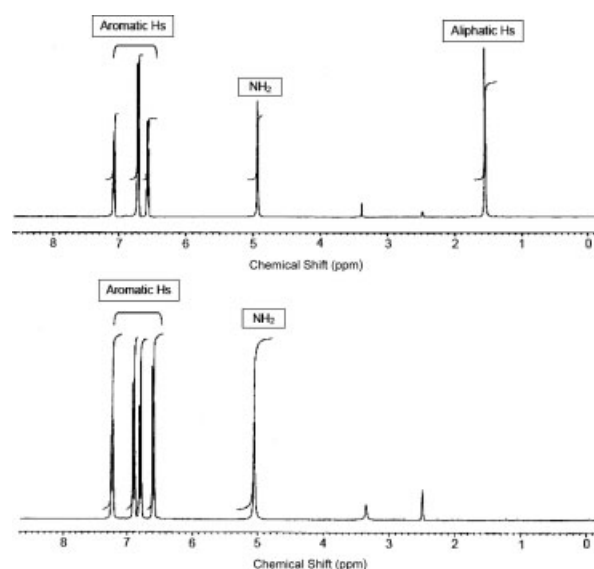
Figure 1 ^{1}H-NMR spectra of BAPP (top) and BAFP (bottom).
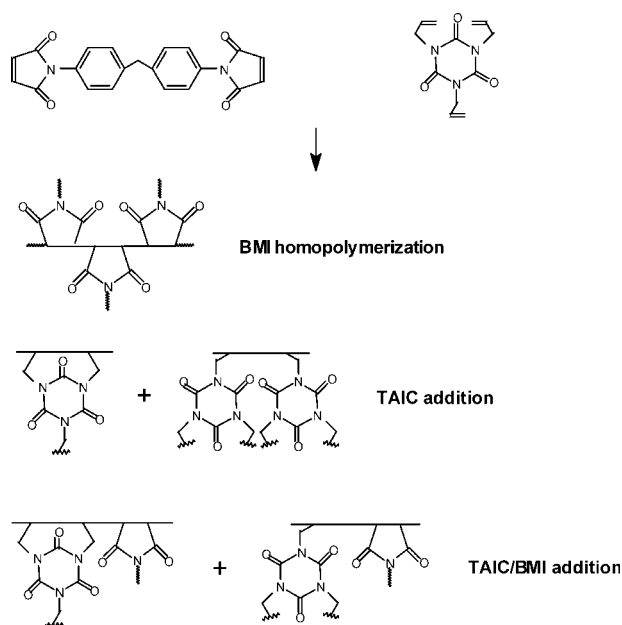
Figure 2 Reaction equation and structure of TAIC/BMI.

tion area of amine Hs/Aromatic Hs is 0.98/3.95 = 1/4.03, which also agrees with the theoretical value of 1/4.0.

Synthesis of copoly(amic acid)

A series of copolyimides containing bisphenol (A or AF) group and siloxane units were synthesized by the conventional two-step method; the synthesis started with diamines and an aromatic tetracarboxylic dianhydride, and these were followed by ring-opening polyaddition and subsequent thermal cyclo-dehydration imidization. The formation of copoly (amic acid) is actually a very complex situation that includes competition between propagation and hydrolysis.[47] According to the Carother's theory, to obtain a high molecular weight copoly(amic acid), the monomer purity and solvent dryness are extremely critical.

## The structure of copolymer

Copolyimide (PIA and PIF)

The reaction is shown in Scheme 1. Although the structures of the copolymers are idealized, most of copolymers contained a small percentage of triads (three mers) in their distributions, because the thermodynamically and spatially preferred structure was usually the dyad configuration (two mers). The composition of the repeating unit differed from that of the two mers (monomeric units) by the elements of water. The copolymers had sequence lengths of one, two, or at most several repeating units.

The interaction of amine-terminated poly(amic acid) with TAIC/BMI

Matsumoto et al.[48–50] have been concerned with the elucidation of the specific polymerization behavior of TAIC. This results from the intermolecular reaction of TAIC on the linear polymer chains. The most important curing reaction of BMI resins has been their homopolymerization[51] at elevated temperatures. BMI resins generally show DSC exothermic peak temperature at around 245°C.[52] The maleimide group can undergo a variety of chemical reaction, and the reactivity of the double bond is a consequence of the electron withdrawing nature of the two adjacent carbonyl groups, which create a very electron-deficient double bond, and therefore is susceptible to homopolymerization. The reactive comonomers of TAIC/BMI have been shown to be quite complex, and the reaction equation is shown in Figure 2. The coreaction can yield combinations of chain extension, branching, and crosslinking depending on the reaction path and state, and the three products are BMI homopolymerization, TAIC addition, and TAIC/BMI addition. The onset temperature of an equivalent mix of TAIC/BMI was around 243°C by DSC as shown in Figure 3-I. However, for the TAIC/BMI-Ph$_3$P system (see Figure 3-II), the onset polymerization peak was shifted to the lower temperature ($\sim$161°C). This can be ascribed to the likelihood that a very small quantity of accelerator (Ph$_3$P) can have a marked effect on the rate of polymerization, and the predominant reaction is chain extension of the double bond between the allyl and maleimide, with negligible reaction between the BMI monomers (higher reaction temperature), and the quick dissolution in DMSO of the resulted TAIC/BMI polymer (200°C reaction) suggested that the reactions of allyl and maleimide groups formed a chain extended copolymer, with the residual double bonds of TAIC or BMI being negligible (steric effect).
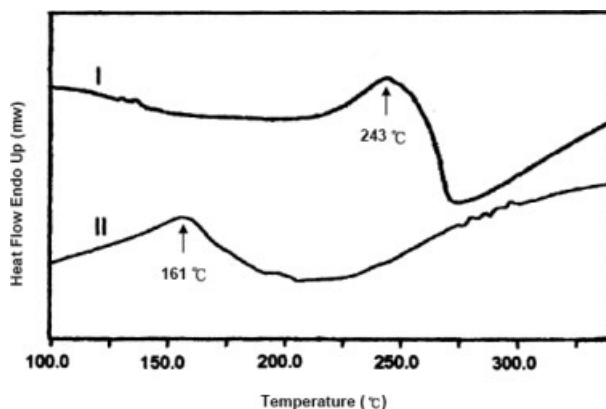
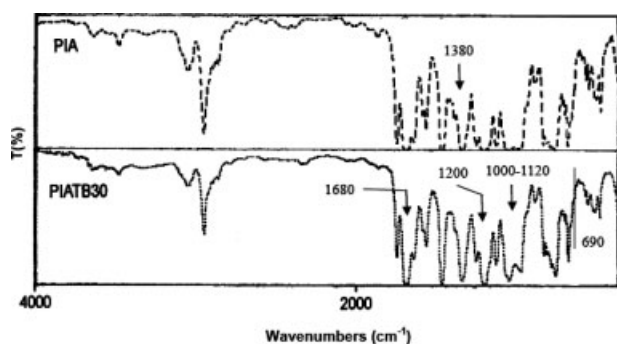**Figure 3** DSC scans for (I) TAIC/BMI and (II) TAIC/BMI-Ph$_3$P.
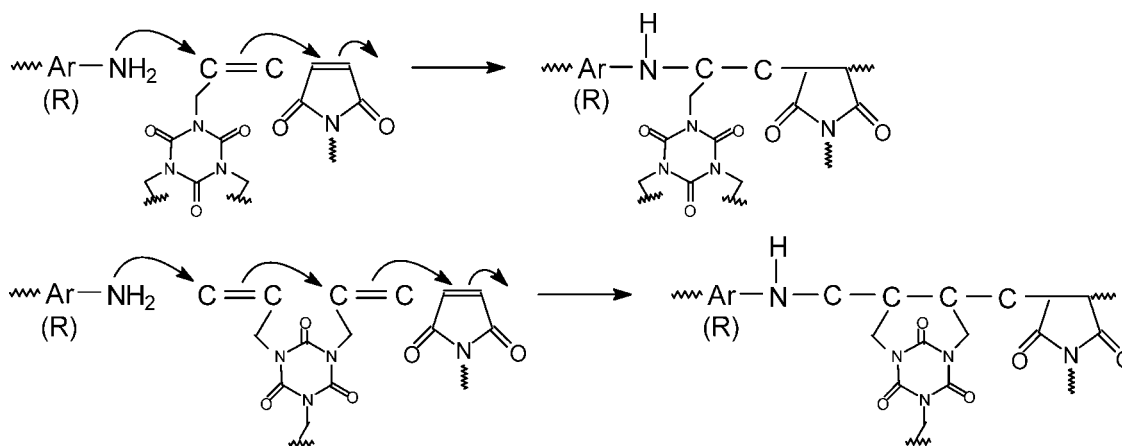
Figure 4 Two possible electrophilic addition of amine-terminated poly(amic acid) with TAIC/BMI.

The section treats cases in which whole polymer chains are linked together to form larger polymer structures. Stated mathematically, the probability of finding a sequence $\cdots ABC \cdots$ of repeating units A, B, C$\cdots$, which can be written

$$P(\cdots ABC \cdots) = P(A)P(B)P(C)$$
$$= \prod_i P(i) \quad i = A, B, C \cdots \quad (3)$$

where the $P(A)$, $P(B)$, $P(C)$ and so forth are the unconditional probabilities of the occurrence of the various repeat units. A suitable amine-terminated oligomer, e.g. ATOS, is coreacted with a monomeric diamine (BAPP or BAFP) and dianhydride (BTDA). Since the initial amine-functionality was supplied by the two diamines (ATOS/BAPP or ATOS /BAFP), as the reaction approaches completion, the chain cleavage might be postulated as a shift in the equilibrium for the poly(amic acid) toward amines, acids, or anhydrides that constitute a competing reaction with each other.[47] The reaction equation is shown in Scheme 2. The possible nucleophilic addition of amine-terminated poly(amic acid) with TAIC/BMI can be expressed as shown in Figure 4.
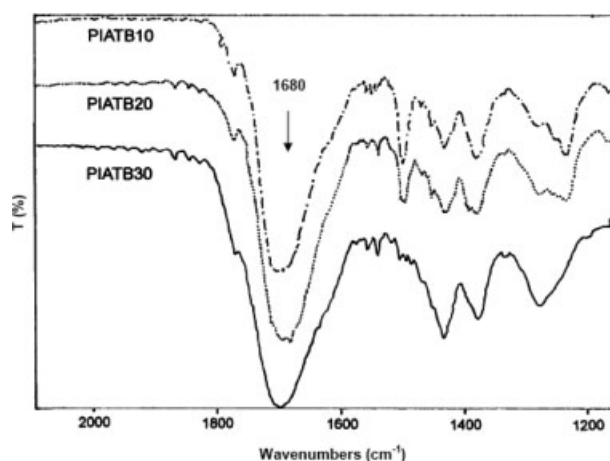
The infrared spectra (in Fig. 5) of PIA and PIATB30 were almost identical, which may be attributed to the similar functional groups in both polymer matrices, the imide structure showed two absorptions at 1770 and 1715 cm^{-1} that are related to symmetric and asymmetric C=O and the absorption at 1380 cm^{-1} is C—N groups, while the characteristic maleimide double bonds at a 690 cm^{-1} had disappeared while the peak assigned to succinimide (C—N—C, 1200 cm^{-1}), which the secondary amine (Ar—NH—C and R—NH—C) showed a medium intensity band at 1000–1120 cm^{-1}. For TAIC/BMI at various mole ratio, if excess TAIC was employed, the peak assigned to allyl (C=C—C—, around 1680 cm^{-1}) had increased to a broad peak around this wavenumber, as shown in Figure 6. If eq. (3) is considered, some of the possible copolymers will be represented by

$$\text{Short sequence} : \text{poly}(A - ran - B - ran - C)$$

The term $-ran-$ was used to indicate a random copolymer.

Figure 5 IR spectra of PIA and PIATB30, the viscous solution was cast onto a glass plate and dried to obtain the film.

Figure 6 IR macrograph spectra of PIATB10, PIATB20, and PIATB30.

Characterization of copolymers

Intrinsic viscosity measurement

The intrinsic viscosities of the polymers in concentrated NMP solutions (i.e. c = 0.12–0.16 g/dL) were measured at 30°C with an Ubbleiohde viscometer. For dilute solutions, the logarithm of relative viscosity is divided by c (concentration) and, extrapolating to zero concentration, yields the intrinsic viscosity, i.e. $\left[\frac{\ln \eta_r}{c}\right]_{c\to 0} = [\eta]_{exp}$, where η_r is the relative viscosity (η / η_0, η: for the solution; η_0: for the solvent).
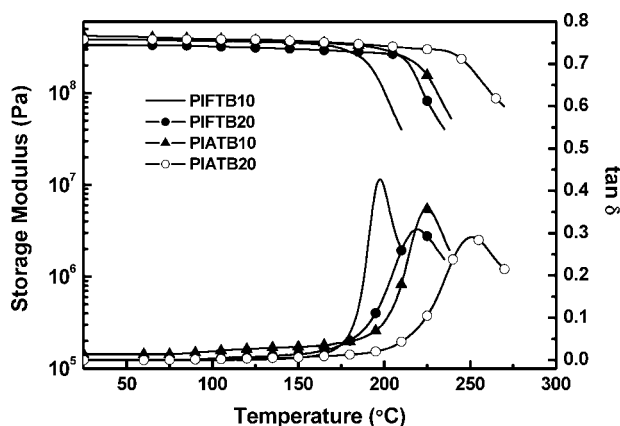
Another calculated method of the intrinsic viscosity, for which the following algebraic expansion is useful;

$$\frac{\ln \eta_r}{c} = \frac{1}{c}\left[(\eta_r - 1) - \frac{1}{2}(\eta_r - 1)^2 + \frac{1}{3}(\eta_r - 1)^3 - \cdots\right]$$
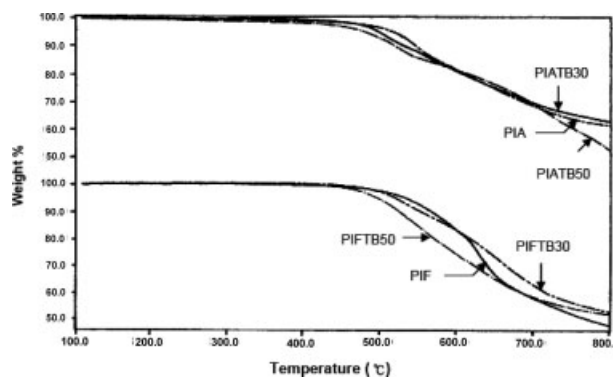$$(0 < \eta_r < 2) \quad (4)$$

For dilute solutions, the full eq. (4) may be written (taking two terms) as

$$\frac{\ln \eta_r}{c} = \frac{1}{c}\left[(\eta_r - 1) - \frac{1}{2}(\eta_r - 1)^2\right]$$
$$= \frac{1}{2c}\eta_r(\eta_r - 1)(3 - \eta_r) = [\eta]_{cal} \quad (5)$$

The intrinsic viscosities will be comparison between experimentally determined data and the calculated values from eq. (5). Table I summarizes the resulted copolyimides. The intrinsic viscosity of copolymers PIA and PIF had experimental values of 0.44 and 0.56, while $[\eta]_{exp}$ values of PIATB and PIFTB systems were from 0.47 to 1.11 and 1.15 to 1.97, respectively. The intrinsic viscosity values of PIATB and PIFTB were much higher than that of PIA and PIF systems, which may be due to lower polymer chain mobility because of the polymer back-

Figure 8 TGA scans of (top) PIA, PIATB30 and PIATB50, (bottom) PIF, PIFTB30 and PIFTB50.

bone having pendant bulky groups. For the PIATB and PIFTB system, the intrinsic viscosity increase with the content of TAIC/BMI, because of the formation of a high-molecular-weight polymer.

DMA and TGA analysis

Figure 7 shows the DMA scans for glass transition temperature (T_g) of PIATB10, PIATB20, PIFTB10, and PIFTB20. The DMA scan of copolymers showed only one T_g, indicating that the various repeating units are randomly distributed along the polymer chain, and form a random copolymer structure, which may be attributed to the amorphous molecular structure for all copolymers. The T_g values of PIFTB system were lower than the PIATB system, and this may be attributed to the decrease in density of molecular chain. Moreover, T_g increased with the

Figure 7 DMA scans for T_g of PIATB10, PIATB20, PIFTB10, and PIFTB20.

TABLE II
Solubility Behavior of Copolyimides

Polymer	Solvent[a]					
	THF	*m*-Cresol	DMF	DMSO	DMAc	NMP
PIA	−	h−	h−	h−	h−	h+
PIATB10	−	h−	h+	h−	h+	h+
PIATB20	−	h−	h−	h+	h−	+−
PIATB30	−	h−	h−	h−	h−	+−
PIATB40	−	h−	h−	h−	h−	+−
PIATB50	−	h−	h−	h−	h−	+−
PIF	−	h−	h−	h−	h−	h+
PIFTB10	−	h−	h+	h+	h+	+−
PIFTB20	−	h−	h+	h+	h+	+−
PIFTB30	−	h−	h−	h+	h−	+−
PIFTB40	−	h−	h−	h−	h−	+−
PIFTB50	−	−	h−	h−	h−	+−

[a] The solubility of copolyimides were measured at a concentration of 1.0 g/dL in solvent. +−, soluble at room temperature, but a few residuum was observed, indicating the very few homopolymerization of BMI; −, insoluble in hot solvent; h+, soluble in hot solvent, but yet a few residuum was observed; h−, swelled or slightly soluble in hot solvent.
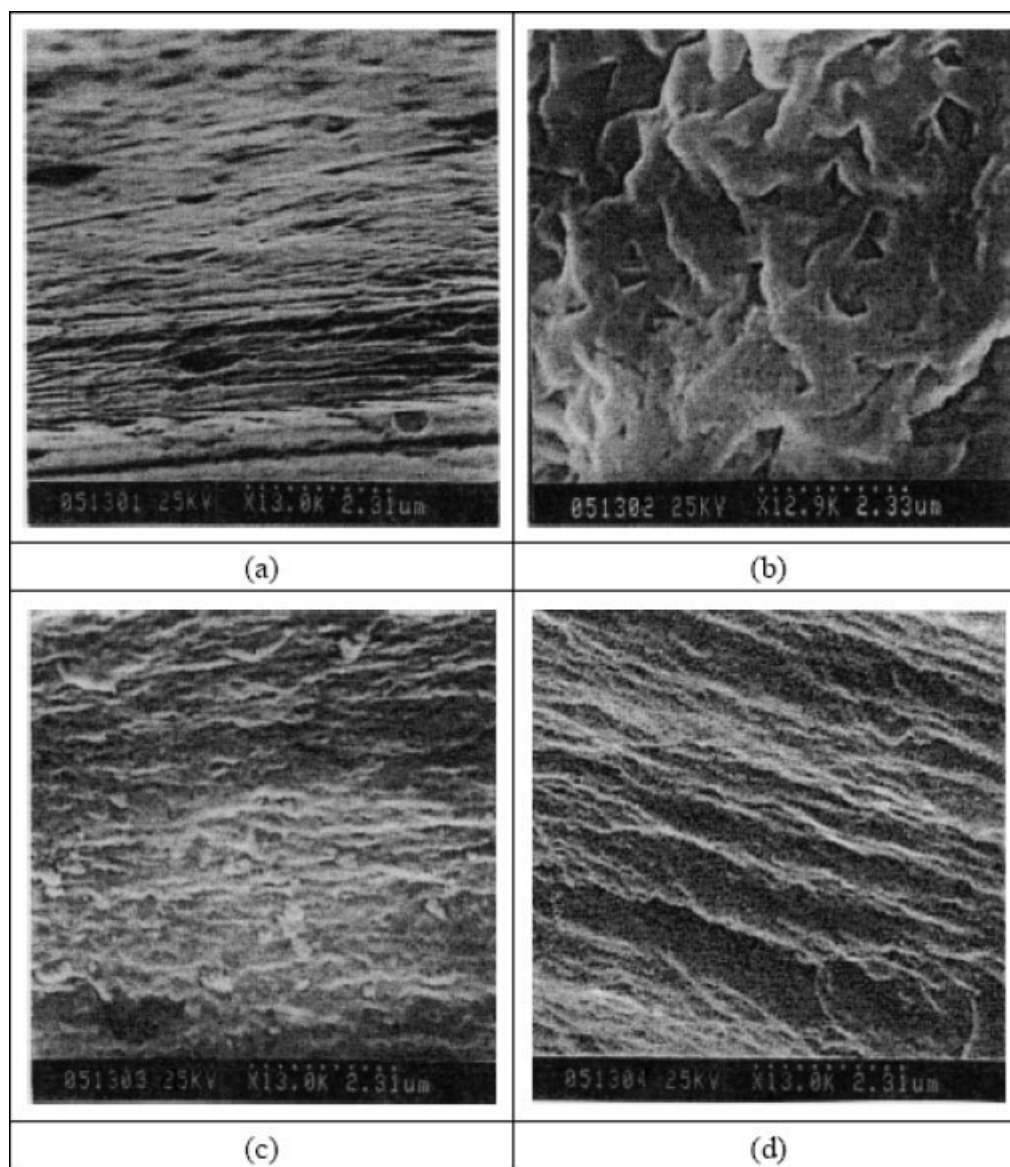
Figure 9 SEM micrographs of the fracture surface of (a) PIATB20, (b) PIATB30, (c) PIFTB20, and (d) PIFTB30.

content of TAIC/BMI (see Table I), and this result may be due to the increase in the concentration of pendant group and stiff structure of polymer chains. The thermal properties of the copolymers were shown in Figure 8. The results of the TGA analyses showed an excellent thermal stability of the synthesized copolymers. The 5 wt % losses in N_2 atmosphere were 483–530°C and the char yields at 800°C were in the range of 51–63% for PIATB system, and the corresponding values were 502–556°C and 51–55% for PIFTB system. For the PIATB system, the 5 wt % degradation temperatures were slightly lower than that of PIFTB system, the reduction of T_d may be attributed to the fact that the C—H bond (degradation energy is 414 kJ/mol) is less stable than the C—F bond (degradation energy is 502 kJ/mol). Table I also lists the modulus values of all the

copolyimides had moderate values. The modulus at 75°C is a functional of TAIC/BMI content, indicating that the coreaction of copoly(amic acid) with TAIC/BMI would promote the rigidity of the resulted copolyimide.

Dielectric constant and dissipation factor

A material with low dielectric constant and dissipation factor will reduce the signal propagating delay time [$t_d = l \times (\sqrt{D_K}/C)$], and the signal propagating loss [$L = K \times (f/C) \times \sqrt{D_K} \times D_f$]. The dielectric constant and dissipation factor of copolyimides are shown in Table I. They (PIATB and PIFTB) were noticeably lower than that the corresponding PIA and PIF. Hougham and coworkers[53,54] report that the dielectric constant can be reduced by increasing
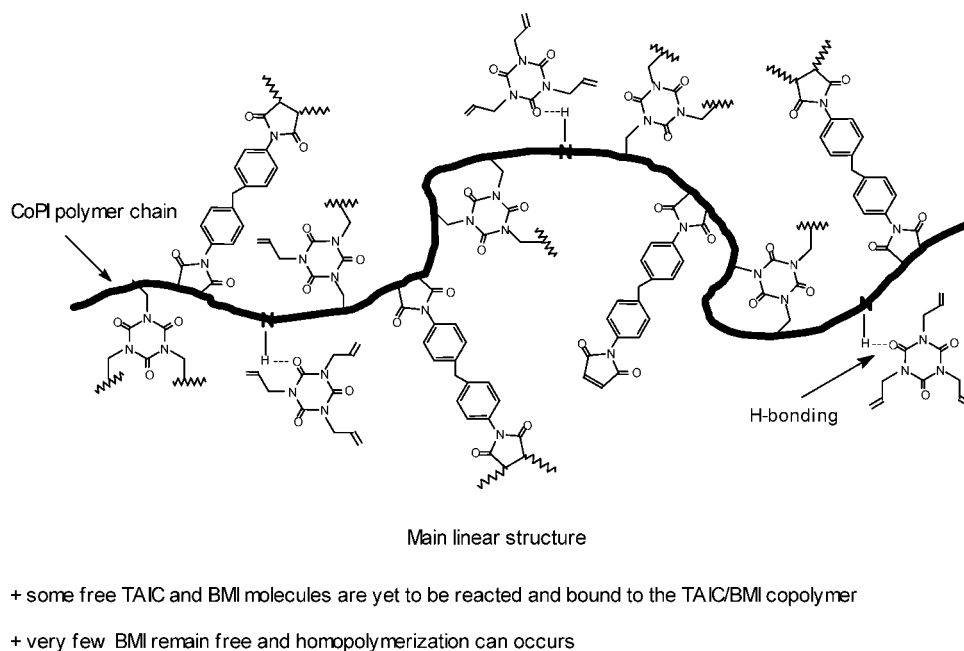
Figure 10 Schematic drawing of the final molecular structure showing the products of the copoly(amic acid) with TAIC/BMI-Ph$_3$P mix system after heating.

the molecule's free volume and by decreasing polarization, The pendant structure have led to greater spacing between polymer molecules and resulted in a less efficient chain packaging and an increase in the free volume of the polymer, thus decreasing the dielectric constant and dissipation factor. From Table I, it can be seen that the dielectric constant decreases with the increase of TAIC/BMI content in the PIATB and PIFTB systems, which indicates TAIC/BMI pendant group has increased free volume of the resulted polymer. Furthermore, for the same content of TAIC/BMI, the fluoropolymers (PIFTB system) exhibited lower dielectric constant than polymer without (PIATB system).

Solubility

Solubility will influence the processability for electronic applications. The solubility of copolymers in various solvents was investigated and the results are summarized in Table II. Copolymer of PIATB systems exhibited somewhat limited solubility, and PIFTB systems show better solubility, because the C—F bond length (~1.36 Å) is larger than that of C—H (1.10 Å). Although, the molecular structure of copolymers PIATB and PIFTB were rather similar, but the molecular volumes were different, PIATB had a smaller free volume which led to a decrease in solubility. Moreover, owing to the introduction of a bulky isocyanurate side group and siloxane segments into the copolymer, they have exhibited a good solubility toward test solvents. Generally, the polymers possess hexafluoroi-

sopropylidene unit[55] and ketone unit between two phthalimide groups[56] on polymer chain, and exhibited high solubility because of the electronic polarizability of its carbonyl group and hexafluoroisopropylidene groups, which hindered the interaction between neighboring molecules.

SEM results

In order to provide a structure and property comparison, the fractured surface of copolymers at various compositions were examined by scanning electron micrographs. Figure 9 shows SEM micrographs of PIATB20, PIATB30 and PIFTB20, PIFTB30 at around 13,000 × magnification. As can be seen, the fracture surface all revealed a simple plane, with no visible phase domains or boundaries. The samples exhibited a homogeneous structure, indicating that a homogeneous state has been achieved in this coreaction system.

From the earlier discussion, the possible final structure of copolymer is depicted in Figure 10. The resulting structure of the copoly(amic acid) with TAIC/BMI after heat-induced reactions, and dehydration has yielded copolyimides. It implies that copolymerization between amine-terminated imide and TAIC/BMI has occurred, which is consistent with the single T_g for the copolyimide observed by DMA.

CONCLUSIONS

The copolyimides containing pendant isocyanurate and siloxane linkage were prepared from copoly

(amic acid), PAA, or PAF with TAIC/BMI. These copolyimides provided excellent physical properties, such as thermal stability, electric properties, and solubility, which meet the essential requirements for high frequency electrical laminate application. The copoly(amic acid) interacts with TAIC/BMI, and then dehydrated at elevated temperature. The copoly (amic acid) formation is actually a very complex situation which includes the intramolecular or intermolecular competition between propagation and hydrolysis, which the reaction can yield combination of chain extension, branching, and crosslinking depending on the heating path. DMA scans of all copolymers showed only one T_g, which indicated that the polymers are a random copolymer structure and the morphology was in good agreement with the proposed molecular structure.

References

1. Lin, C. H.; Cai, S. X.; Leu, T. S.; Hwang, T. Y.; Lee, H. H. J Polym Sci Part A: Polym Chem 2006, 44, 3454.
2. Lin, C. H.; Yang, K. Z.; Leu, T. S.; Lin, C. H.; Sie, J. W. J Polym Sci Part A: Polym Chem 2006, 44, 3487.
3. Cai, S. X.; Lin, C. H. J Polym Sci Part A: Polym Chem 2005, 43, 2862.
4. Lin, C. H.; Cai, S. X.; Lin, C. H. J Polym Sci Part A: Polym Chem 2005, 43, 5971.
5. Stenzenberger, H. D.; Wilson, D. Polyimides; Blackie: Glasgow, 1990; Chapter 7.
6. Sek, D.; Pijet, P.; Wanic, A. Polymer 1992, 33, 190.
7. Yang, C. P.; Chen, W. T. J Polym Sci Part A: Polym Chem 1993, 31, 2799.
8. Moy, I.; Konas, T. M.; McGrath, J. E.; Fields, E. K. J Polym Sci Part A: Polym Chem 1994, 27, 2377.
9. Volksen, W.; Hergenrother, P. M. High Performance Polymers; Springer: Berlin, 1994; p 111.
10. Leu, T. S.; Wang, C. S. Polymer 2002, 43, 7069.
11. Yen, C. T.; Chen, W. C.; Liaw, D. J.; Lu, H. Y. Polymer, 2003, 44, 7079.
12. Wahab, M. A.; Kim, I. L.; Ha, C. S. J Polym Sci Part A: Polym Chem 2004, 42, 5198.
13. Reddy, D. S.; Shu, C. F.; Wu, F. I. J Polym Sci Part A: Polym Chem 2002, 40, 262.
14. Chou, C. H.; Reddy, D. S.; Shu, C. F. J Polym Sci Part A: Polym Chem 2002, 40, 3615.
15. SL, N. H.; Chen, Z. K.; Huang, W.; Xu, Y. S.; Cao, Y. J Polym Sci Part A: Polym Chem 2004, 42, 1647.
16. Kim, Y. H.; Kim, H. S.; Kwon, S. K. Macromolecules 2005, 38, 7950.
17. Ghatge, N. D.; Shinde, B. M.; Mulik, U. P. J Polym Sci Part A: Polym Chem 1984, 22, 3359.
18. Imai, Y.; Maldar, N. N.; Kakimoto, M. J Polym Sci Part A: Polym Chem 1989, 22, 2189.
19. Jeong, H. J.; Kakimoto, M.; Imai, Y. J Polym Sci Part A: Polym Chem 1991, 29, 1691.
20. Jeong, H. J.; Oishi, Y. Kakimoto, M.; Imai, Y. J Polym Sci Part A: Polym Chem 1991, 29, 39.
21. Falcigno, P. A.; Jasne, S.; King, M. J Polym Sci Part A: Polym Chem 1992, 30, 1433.
22. Misra, A. C.; Tesoro, G.; Hougham, G.; Pendharkar, S. M. Polymer 1992, 33, 1078.
23. Oishi, Y.; Ishida, M.; Kakimoto, M.; Imai, Y.; Kurosaki, T. J Polym Sci Part A: Polym Chem 1992, 30, 1027.
24. Trofimenko, S.; Auman, B. C. Macromolecules 1994, 27, 1136.
25. Eastmond, G. C.; Paprotny, J. Macromolecules 1995, 28, 2140.
26. Chern, Y. T.; Shiue, H. C. Macromolecules 1997, 30, 4646.
27. Chuang, K. C.; Kinder, J. D.; Hull, D. L.; McConville, D. B.; Youngs, W. J. Macromolecules 1997, 30, 7183.
28. Zheng, H. B.; Wang, Z. Y. Macromolecules 2000, 33, 4310.
29. Chung, I. S.; Kim, S. Y. Macromolecules 2000, 33, 3190.
30. Hasegawa, M.; Sensui, N.; Shindo, Y.; Yokota, R. Macromolecules 1999, 32, 387.
31. Farr, I. V.; Kratzner, D.; Glass, T. E.; Dunson, D.; Ji, Q.; Mcgrath, J. E. J Polym Sci Part A: Polym Chem 2000, 38, 2840.
32. Hergenrother, P. M.; Watson, K. A.; Smith, J. G.; Connell, J. W.; Yokota, R. Polymer 2004, 45, 5441.
33. Sasaki, T.; Moriuchi, H.; Yano, S.; Yokota, R. Polymer 2005, 46, 6968.
34. Yasashima, Y.; Kumada, H.; Yamamoto, K.; Akutsu, F.; Naruchi, K.; Miura, M. Polymer 1995, 36, 645.
35. Akutsu, F.; Saito, G.; Miyamoto, M.; Kasashima, Y.; Inoki, M.; Naruchi, K. Makromol Chem Phys 1996, 197, 2239.
36. Hsiao, S. H.; Lin, K. H. J Polym Sci Part A: Polym Chem 2005, 43, 331.
37. Hergenrother, P. M.; Bryant, R. G.; Jensen, B. J.; Havens, S. J. J Polym Sci Part A: Polym Chem 1994, 32, 3061.
38. Hergenrother, P. M.; Smith, J. W. Polymer 1994, 35, 4857.
39. Simone, C. D.; Scola, D. A. Macromolecules 2003, 36, 6780.
40. Shiobara, T.; Okuse, S.; Aoki, T.; Kato, H. U.S. Pat. 6,143,423 (2000).
41. Kumar, A. A.; Alagar, M.; Rao, R. Polymer 2002, 43, 693.
42. Wu, C. S.; Liu, Y. L.; Hsu, K. Y. Polymer 2003, 44, 565.
43. Wu, S. J.; Lin, T. K.; Shyu, S. S. J Appl Polym Sci 2000, 75, 26.
44. Wu, S. J.; Tung, N. P.; Lin, T. K.; Shyu, S. S. Polym Int 2000, 49, 1452.
45. Leu, T. S. J Appl Polym Sci 2006, 102, 2470.
46. Leu, T. S.; Wang C. S. J Appl Polym Sci 2003, 87, 945.
47. Leu, T. S.; Wang, C. S. J Polym Sci Part A: Polym Chem 2001, 39, 4139.
48. Matsumoto, A.; Matsumoto, T.; Inoue, H.; Oina, M.; Saito, H. Eur Polym J 1990, 26, 661.
49. Matsumoto, A.; Hirai, F.; Sumiyama, Y.; Aota, H.; Takayama, Y.; Kameyama, A.; Nakanishi, T. Eur Polym J 1999, 35, 195.
50. Matsumoto, A.; Watanabe, H.; Aota, H.; Takayama, Y.; Kameyama, A.; Nakanishi, T. Polymer 2000, 41, 3883.
51. Wang, C. S.; Leu, T. S.; Hsu, K. R. Polymer 1998, 39, 2921.
52. Wang, C. S.; Hwang, H. J. J Polym Sci Part A: Polym Chem 1996, 34, 1493.
53. Misra, A. C.; Tesoro, G.; Hougham, G.; Pendharkar, S. M. Polymer 1992, 33, 1078.
54. Hougham, G.; Tesoro, G.; Shaw, J. Macromolecules 1994, 27, 3642.
55. Friring, A. E.; Auman, B. C.; Wonchoba, E. R. Macromolecules 1993, 26, 2779.
56. Yang, C. P.; Chen, W. T. Macromolecules 1993, 26, 4865.